ARKIV FÖR FYSIK Band 14 nr 8

Communicated 23 April 1958 by MANNE SIEGBAHN and ERIK HULTHÉN

On the *L*-Auger lines in the beta-ray spectrum of the active deposit of thoron

By ZIEMOWID SUJKOWSKI[1] and HILDING SLÄTIS

With 5 figures in the text

1. Introduction

A detailed consideration of the problems concerning the Auger electrons as well as a review of theoretical and experimental works on the Auger effect up to 1952 was given by Burhop [1]. Some characteristic features of importance for the interpretation of experimentally recorded Auger lines will be pointed out here.

If we denote by UVW an electron emitted from the W-shell due to the filling of a vacancy in the U-shell by an electron from the V shell, the energy E of this electron is given by:

$$E_{\mathrm{UVW}} = \mathrm{U}_Z - \mathrm{V}_Z - \mathrm{W}(\mathrm{V}_Z)$$

where U_Z, V_Z are the ionization energies in the shells U and V of an atom Z, respectively, and $W(\mathrm{V}_Z)$ is the ionization energy in the W shell of an atom Z already ionized in the V shell.

There is relatively very little experimental data concerning the ionization energy of ionized atoms; some information may be given by the observations of the X-rays satellites. There is also a lack of theoretical data for the heavy elements. Generally we can expect that

$$\mathrm{W}_Z < \mathrm{W}(\mathrm{V}_{Z'}) < \mathrm{W}_{Z+1}.$$

Bergström and Hill [2] introduced the quantity ΔZ, called the effective incremental charge and defined it as follows:

$$\Delta Z = \frac{\mathrm{W}(\mathrm{V}_{Z'}) - \mathrm{W}_Z}{\mathrm{W}_{Z+1} - \mathrm{W}_Z}.$$

Hence

$$E_{\mathrm{UVW}} = \mathrm{U}_Z - \mathrm{V}_Z - \mathrm{W}_{Z+\Delta Z}.$$

This way of computing the number and the electron energy of the possible Auger transitions, although used in most of the works dealing with these problems, has, however, only an approximate character. First of all the interaction between electrons is neglected. This is justified only in the case of pure spin-orbit coupling (*j-j* coupling) for any electron, the mutual interaction between the electrons being neglected. Ference [3] in 1937 discussed the possible configurations for the *KLL*-Auger transitions taking into account the electron-electron interactions. Recently Sokolowski *et al.* [4] renewed this discussion in order to give an interpretation to their experimental results on the *KLL*-Auger electrons produced by the X-rays in copper. For heavy elements, however, e.g. thallium and bismuth which we are dealing with, the influence of the electron-electron interaction seems to be somewhat less important. Apart from this, considering the fact that the *L*-Auger spectra are very complicated, such a discussion for the *L*-Auger electrons would be rather hopeless. Even for simple *KLL* spectra one can theoretically predict only the relative displacement of the lines [4], since the accuracy of the wave functions which are necessary to calculate the absolute energy of the state is so far very poor. Therefore, in the further discussion we shall proceed in the "classical" way, disregarding the influence of the electron-electron interaction. We consider this to be a satisfactory approximation for heavy elements.

---

[1] On leave from the "Instytut Badań Jądrowych", Warszawa.

The characteristic X-radiation emitted as a secondary effect of a radioactive decay has been investigated several times [1]. There is also a great deal of information, experimental as well as theoretical, concerning the *K*-Auger electrons, see for instance ref. [5]. As regards the *L*-Auger electron spectra, however, the data are still incomplete, mainly because the investigation of low energy electrons (5–16 keV for the highest atomic numbers) as yet is very tedious and requires a special technique. Also the theoretical interpretation of these spectra is much more difficult than that of the comparatively simple *K*-Auger spectra.

A knowledge of the Auger effect will always be of importance for the X-ray physics as well as for the study of nuclear radiations.

2. Earlier works on *L*-Auger electrons

L-Auger lines were first investigated by Black [6] in 1925. He recorded the lines from a RaB source on Schumann plates in a semicircular beta-ray spectrometer, and observed 14 lines in the energy region considered. One line was interpreted as an external conversion line in the platinum backing of the source and eleven lines as photo electrons ejected by X-rays ($L\alpha_1$, $L\beta_1$ and $L\gamma_1$) in bismuth. The electronic shells responsible for the origin of the photolines were also given.

Apart from this Black made also a comparison of these results with the lines from a ThB source in equilibrium with its decay products. Since ThC, which is mainly responsible for the *L*-Auger electrons in the latter case, and RaE, being an emitter of *L*-Auger electrons in a RaB source, are isotopes of the same element, $_{83}$Bi, one could expect the same lines in both spectra. This comparison confirmed the ascription of the experimentally found lines to the element $Z = 83$, although the author was not certain of this second experiment.

In 1939 Flammersfeld [7] investigated the electron lines from ThB + C + C″ using a semicircular magnetic beta-ray spectrometer with a GM-detector. The resolution of the equipment, however, was not high enough for low energies. He found four lines in the energy region of interest.

Lately several new works on the *L*-Auger spectra appeared. In 1950 Butt [8] investigated the *L*-Auger spectrum of ThB + C + C″ using a post-focusing acceleration method in a magnetic lens beta-ray spectrometer with a GM-detector. He found

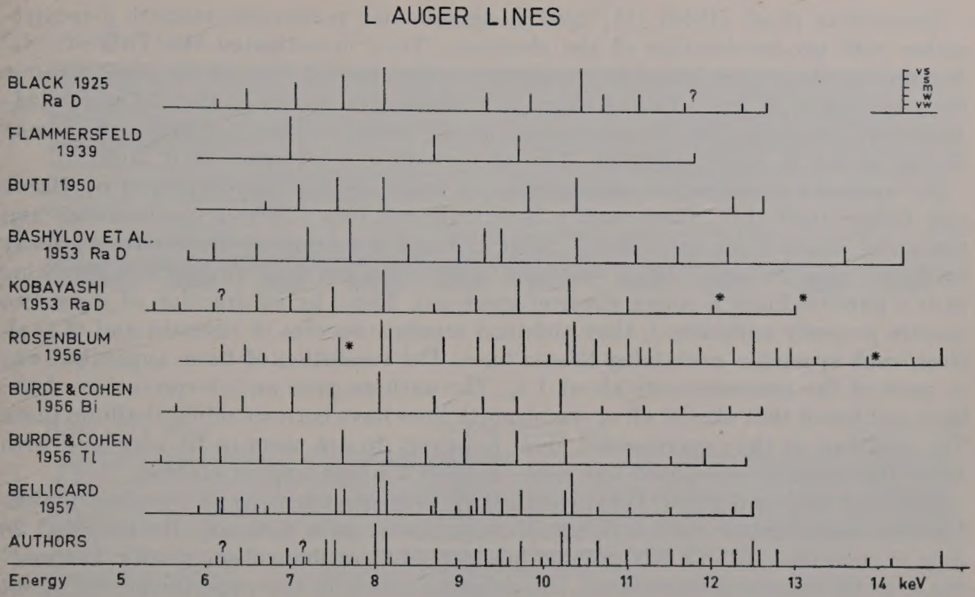

Fig. 1. Comparison of the *L*-Auger lines in the beta-ray spectrum of ThB + C + C″, recorded by different authors. vs = very strong, s = strong, m = medium, w = weak, vw = very weak, * = unresolved band. The positions of the Auger lines are marked by vertical lines, the lengths of which indicate the visually estimated intensities.

eight lines, five of which he ascribed to bismuth ($Z = 83$) and three to thallium ($Z = 81$). The resolution in his spectrometer, however, was still insufficient for investigating such complicated spectra. Also the post-focusing electron acceleration method (used in order to diminish absorption losses in the counter window of 0.4 mg/cm² thickness) and the platinum backing causing strong back-scattering, decreased the precision of the measurements.

The works of Kobayashi (1953) [9] and Bashylov *et al.* (1953) [10] are also of interest in this review of earlier investigations. Kobayashi investigated the radioactive decay of RaD with a spherical condenser-type electrostatic spectrometer with a resolving power of 1.3 %. He found 12 lines which he interpreted as RaE *L*-Auger lines (bismuth), two uninterpreted bands at 11.7–12.6 and 12.6–13.5 keV respectively, and also a band at 15–16 keV interpreted as a conversion line and at 4–5 keV, not so certain, also suggested to be a conversion line. The agreement between the positions of these lines from RaE and those of ThC lines found in other experiments is quite good (see Fig. 1). Although there is another mode of excitation also the intensity ratios of the corresponding lines are similar, at least as regards the strongest ones.

Bashylov *et al.* [10] investigated the conversion spectrum of RaD using a magnetic spectrometer called "Ketron" by the authors, with focusing in an ununiform field. The Auger electrons were investigated rather marginally. The authors found 16 lines in the *L*-Auger electron energy region (from 5.8 to 14.3 keV) but did not interpret them. The accuracy of their measurement, however, was not very good in this energy region and the positions of their lines do not agree with any other experiment, as is seen from Fig. 1.

Rosenblum *et al.* (1956) [11] used a semicircular permanent-magnet β-spectrometer with pre-acceleration of the electrons. They investigated the ThB + C + C″ *L*-Auger spectrum and found in the photographic plate 31 lines in the energy region from 6.20 to 14.76 keV. Two of them were unresolved bands (7.43–7.73 and 13.51–14.23 keV, respectively). They observed also a band between 1–3 keV, which may belong to the *M*-Auger spectrum. The authors did not interpret their lines.

An interesting method of investigation of these spectra was employed by Burde and Cohen 1956 [12]. They used a thin magnetic lens electron spectrometer and measured, apart from the "usual" total *L*-Auger spectrum of ThB with its decay products, also the coincidence spectrum with alpha particles from ThC, obtaining thus a pure thallium *L*-Auger electron spectrum. Then, by subtraction of these two spectra properly normalized, they obtained separate spectra of bismuth and of thallium, each spectrum containing fifteen lines. The resolution of their apparatus was in most of the measurements about 1 %. The authors gave an interpretation of the lines and found that almost all of the bismuth lines have corresponding thallium lines. The positions of the experimental lines, however, do not seem to fit very well with those theoretically computed but agree only in a rough approximation.

Recently Bellicard (1957) [13] investigated these spectra using an iron-free double-focusing spectrometer with a Geiger-Müller counter as a detector. He recorded 26 lines of energies 5.920–12.500 keV and interpreted 21 of them theoretically. Estimating from the spectrum reproduced, the resolving power in this experiment was about 0.5 %. The position and the intensity (our estimation) of the lines is seen in Fig. 1.

3. Experimental methods

(*a*) *Spectrometer*

The Auger lines were recorded in the 45 gauss permanent magnet beta-ray spectrometer recently described by Slätis [14]. The resolution used was better than 1 pro mille.

(*b*) *Sample*

The sample consisted of the well-known thoron active deposit, collected on a carbonum wire (diameter 0.13 mm, length 8 mm) by the usual method of keeping the wire at a high negative voltage over a radiothorium source. This "activation" of the carbonum wire was performed over 24 hours. The strength of the activity was then about 500 μC. Carbonum was used in order to reduce the back-scattering and in order to prevent external conversion electrons coming from the backing. In the case of thoron active deposit (and similar for radon and actinon deposits) the activity has the character of a monolayer. This circumstances is very advantageous for the study of low energy electrons such as the Auger electrons, because no broadening arising from absorption in the active layer occurs.

(*c*) *Plates*; *expositions*

No *L*-Auger lines are usually observed on the common films—such low energy electrons stop already in the protecting layer of the emulsion. Also the ordinary one-day exposure is by far insufficient for an investigation of very weak but numerous lines. Therefore two different many-days exposures were carried out in which a new-activated wire was inserted in the spectrometer every day. For this purpose two similar carbon wires in similar holders were employed. While one of the wires was

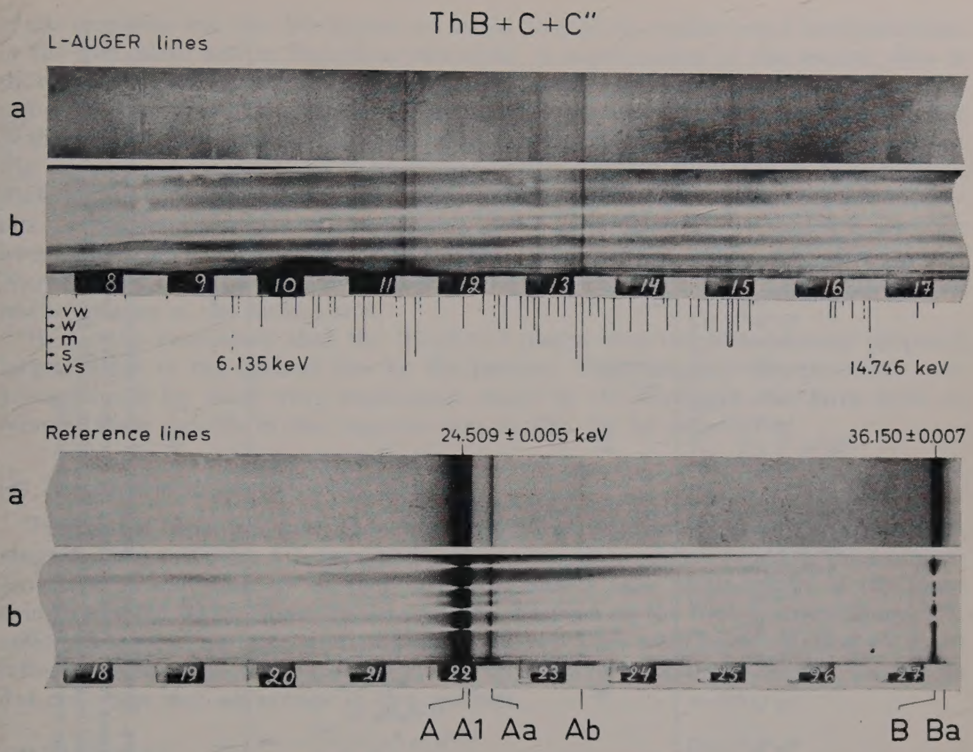

Fig. 2. *L*-Auger lines in the beta-ray spectrum of ThB + C + C″. Compare the text of Fig. 1. The active deposit was on a carbonum wire, diameter 130 μ, length 8 mm. Two similar wires were used alternately. While one of the wires was activated, the other one was used in the spectrometer. (*a*) Ilford Nuclear Research Emulsion G-5, 5 μ thick, exposure 7 weeks. (*b*) Ilford Nuclear Research Emulsion in Gel Form, G-5, the plates prepared at our Institute [14], exposure 3 weeks. The energy values for the reference lines *A* and *B* are given in ref. [16].

being activated the second one was used in the spectrometer. In the first twenty days exposure the plate used was prepared with "Ilford Nuclear Research Emulsions in Gel Form, G.5", and the emulsion was made as thin as possible. (The range of the electrons of the *A*-line in the ThB + C + C″ conversion electron spectrum, used for a calibration line, is in Ilford G-5 emulsion slightly above 4 μ; the range of the *L*-Auger electrons, which is of interest, is between 1 and 3 μ. See Gauthé and Blum [15]). This is of as great or even more importance from the point of view of reducing the background (mainly from X- and γ-rays) as of reducing the fixing time. As the range of so weak electrons in an emulsion is extremely short, some very weak lines may be completely destroyed in the fixing process, since the silver in the external layer of the emulsion is dissolved in the fixing bath. It was observed that weak lines in this energy region, which were seen when the fixation started disappeared after some minutes.

After the first long-time exposure (see Fig. 2*b*) it was decided to make a new one with a radiation dose of two times the first one. This time we decided to use the Ilford Nuclear Emulsion plate of the G-5 type, prepared by the factory. The thickness

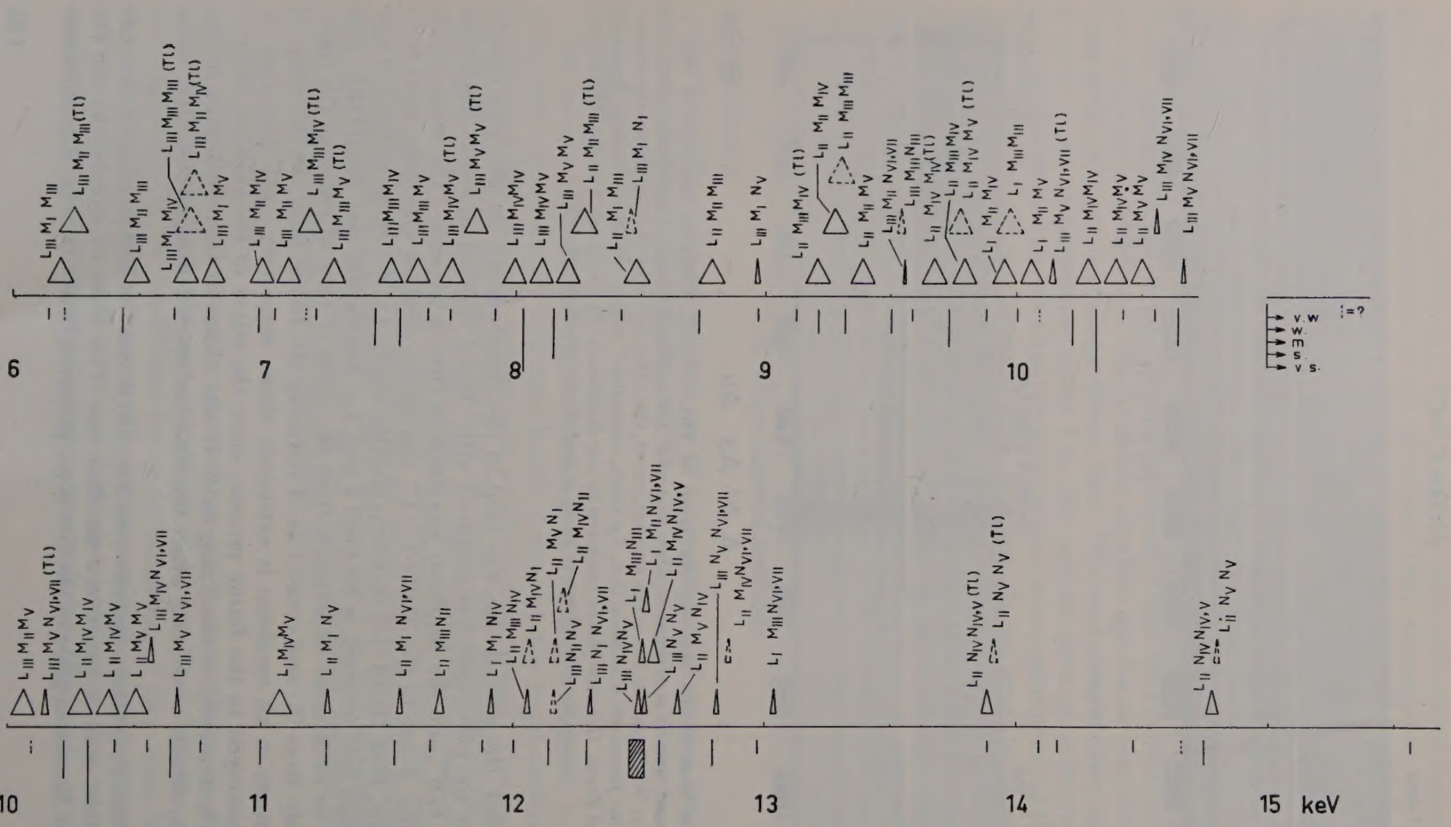

Fig. 3. Interpretation of the *L*-Auger lines found by the present authors. The right hand end point of the basis of a triangle corresponds to an *LVW* energy obtained by subtracting the V- and W-ionization energies from the *L*-energy, all energies taken for the same *Z*-value. The left hand end point of the triangle basis corresponds to an energy obtained in a similar way, the ionization energy for the W-shell, however, taken for the value $Z+1$. As to the size of the vertical lines, see the text to Fig. 1.

of the emulsion was 5 μ. We hoped we would be able to confirm some uncertain lines in the first plate and to find some new ones. A reproduction of the second plate is shown in Fig. 2*a*. Strangely enough the lines on this industrially prepared plate are not to be seen as clearly as those on the earlier plate. In spite of the inhomogeneities of the emulsion thickness on the first plate and the shorter exposure dose the lines in Fig. 2*b* are both stronger and sharper than the lines in Fig. 2*a*. (It may be mentioned that the inhomogeneity of the emulsion thickness of the plate of Fig.2*b* is advantageous for the determination of the position of the calibration line *A*, which is strongly overexposed in the thicker parts of the emulsion, but not in the very thin layers.) Nevertheless we excluded some uncertain lines, found in the first plate, which were not to be seen in the second one.

It may be mentioned that the Ilford G-5 plates were cut from already prepared larger plates in the desired size by the factory. Unfortunately this procedure was accompanied by some very unpleasant stains in the emulsion. We have tried to remove these defects in the reproduction in Fig. 2*a* by retouching.

(*d*) *Preparation of copies of the plates*

The plates obtained were then investigated in two ways. At first photographic magnifications in ratio 4:1 were made. More than 40 lines were found in these copies. However, it appeared to be very advantageous to take photographs of the plate using reflected light. Some uncertain lines observed on the first mentioned magnifications appeared quite prominently and some new lines were found. Making copies in reflected light when the plate was placed on a mirror was also tried, but the results did not show any advantage in this method.

(*e*) *Calibration*

The well known *A* line of the Th(B + C + C″) β-ray spectrum was used for the calibration. The value of this line was taken from Siegbahn and Edvarson [16] as (534.20 ± 0.06) gauss · cm or (24.503 ± 0.005) keV. The determination of the 2ϱ-values of the lines was performed in the way previously described [14, 17].

4. Experimental results

54 lines were finally found in the energy region considered. At least one of them (about 12.500 keV) should be considered to be an unresolved band. Our results, together with the interpretation of the transitions (see below), are given in Table 1, and also, for convenience, in Figs. 1 and 3. The triangles in Fig. 3 denote the possible variation of ΔZ from 0 to 1. In Table 1, however, we give the theoretical energy values only for $\Delta Z = 1$. It is immediately seen already from Fig. 3 without any additional assumption that this approximation is quite satisfactory. Table 2 and, as mentioned above, Fig. 1 show a comparison of our results with those of earlier workers. As the highest resolution so far for these Auger lines is used by us, our energy values given in Table 1 might also be the most accurate. The more accurate the energy values are, the safer one is in the interpretation of the transitions responsible for the lines in question. As a matter of fact the fluctuations of the differences between the experimental and the computed energy values are in our case the smallest ones. As regards the intensities, however, we were able only to estimate them visually. As the photo-

Table 1. Results and interpretation of the *L*-Auger lines found in the present work.

v.s. = very strong, s = strong, m = medium, w = weak, v.w. = very weak.

No.	Energy (keV)	Transition	Energy (computed) (keV)	Intensity
1	6.135	$L_{III} M_{I} M_{III}$	6.129	v.w.
2	6.197	$L_{III} M_{II} M_{III}$ (Tl)	6.174	?
3	6.429	$L_{III} M_{II} M_{III}$	6.430	w.
4	6.636	$L_{III} M_{I} M_{IV}$	6.629	v.w.
		$L_{III} M_{II} M_{IV}$ (Tl)	6.658	v.w.
5	6.773	$L_{III} M_{I} M_{V}$	6.739	v.w.
6	6.970	$L_{III} M_{II} M_{IV}$	6.930	w.
		$L_{III} M_{III} M_{III}$	6.947	w.
7	7.033	$L_{III} M_{II} M_{V}$	7.040	v.w.
8	7.157	$L_{III} M_{III} M_{IV}$ (Tl)	7.118	?
9	7.197	$L_{III} M_{III} M_{V}$ (Tl)	7.223	v.w.
10	7.434	$L_{III} M_{III} M_{IV}$	7.447	m.
11	7.535	$L_{III} M_{III} M_{V}$	7.557	m.
12	7.644	$L_{III} M_{IV} M_{V}$ (Tl)	7.692	v.w.
13	7.735	$L_{III} M_{V} M_{V}$ (Tl)	7.789	v.w.
14	7.911	$L_{III} M_{IV} M_{IV}$	7.939	v.w.
15	8.025	$L_{III} M_{IV} M_{V}$	8.049	v.s.
16	8.147	$L_{III} M_{V} M_{V}$	8.157	s.
17	8.198	$L_{II} M_{II} M_{III}$ (Tl)	8.210	v.w.
18	8.417	$L_{II} M_{I} M_{III}$	8.425	v.w.
19	8.732	$L_{II} M_{II} M_{III}$	8.726	w.
20	8.967	$L_{III} M_{I} N_{V}$	8.951	v.w.
21	9.120	$L_{II} M_{III} M_{IV}$ (Tl)	9.154	v.w.
22	9.207	$L_{II} M_{II} M_{IV}$	9.226	w.
23	9.316	$L_{II} M_{II} M_{V}$	9.336	w.
24	9.499	$L_{III} M_{II} N_{VI,\,VII}$	9.549	w.
		$L_{III} M_{III} N_{III}$	9.525	w.
25	9.585	$L_{II} M_{IV} M_{IV}$ (Tl)	9.623	v.w.
26	9.729	$L_{II} M_{III} M_{IV}$	9.743	m.
		$L_{II} M_{IV} M_{V}$ (Tl)	9.728	m.
27	9.878	$L_{I} M_{II} M_{IV}$	9.901	v.w.
28	9.998	$L_{I} M_{II} M_{V}$	10.011	v.w.
29	10.087	$L_{III} M_{V} N_{VI,\,VII}$ (Tl)	10.129	v.w.
30	10.223	$L_{II} M_{IV} M_{IV}$	10.235	m.
31	10.315	$L_{II} M_{IV} M_{V}$	10.345	v.s.
32	10.423	$L_{II} M_{V} M_{V}$	10.452	v.w.
33	10.547	$L_{III} M_{IV} N_{VI,\,VII}$	10.548	v.w.
34	10.643	$L_{III} M_{V} N_{VI,\,VII}$	10.655	m.
35	10.761	*?*		v.w.
36	10.996	$L_{I} M_{IV} M_{V}$	11.020	w.
37	11.257	$L_{II} M_{I} N_{V}$	11.247	w.

Table 1 *(continued)*

No.	Energy (keV)	Transition	Energy (computed) (keV)	Intensity
38	11.529	$L_{II}\ M_{I}\ N_{VI,\,VII}$	11.534	w.
39	11.669	$L_{II}\ M_{III}\ N_{II}$	11.685	v.w.
40	11.874	$L_{I}\ M_{I}\ N_{IV}$	11.897	v.w.
41	11.999	$L_{II}\ M_{III}\ N_{IV}$	12.040	v.w.
42	12.141	$L_{II}\ M_{V}\ N_{I}$	12.146	w.
		$L_{III}\ N_{II}\ N_{V}$	12.144	w.
43	12.289	$L_{III}\ N_{I}\ N_{VI,\,VII}$	12.235	w.
44	12.462–			m.
	12.518			m.
45	12.582	$L_{II}\ M_{V}\ N_{IV}$	12.639	w.
46	12.793	$L_{III}\ N_{V}\ N_{VI,\,VII}$	12.794	w.
		$L_{II}\ M_{IV}\ N_{VI,\,VII}$	12.844	w.
47	12.972	$L_{I}\ M_{III}\ N_{VI,\,VII}$	13.027	v.w.
48	13.885	$L_{II}\ N_{IV}\ N_{IV,\,V}$ (Tl)	13.874	v.w.
		$L_{II}\ N_{V}\ N_{V}$ (Tl)	13.892	v.w.
49	14.091			v.w.
50	14.163			v.w.
51	14.465			v.w.
52	14.656			v.w.
53	14.746	$L_{II}\ N_{IV}\ N_{IV,\,V}$	14.754	w.
		$L_{II}\ N_{V}\ N_{V}$	14.783	w.
54	15.574			v.w.

graphic yield of the photographic emulsion changes quite fast with the energy of the electrons in this energy region, this estimation gives only rough information and must not be used for any quantitative comparison. The intensities of the lines of the other workers, given in Fig. 1 and in Table 2, are either estimated by the authors in the same way as ours (Black, Rosenblum), or estimated by us on the base of distribution curves given by the authors (Butt, Bellicard, Bashylov) or, at last, converted into our five-degree scale from the intensity values given by the authors (Flammersfeld, Burde and Cohen, Kobayashi). Of course in such a procedure the intensity ratios are only approximately maintained but for our illustration purposes and for recognition of the corresponding lines it seems to be sufficient.

The experimental $B\varrho$-values were converted into energy values by interpolation of the values given in the tables of Landolt and Börnstein [18]. To check the values so obtained we computed the energy values for some lines using the exact formula and newer atomic constants [19]. We found differences of about 2–3 eV. The ionization energy values for different atomic shells were taken from Sandström [20]. In order to calculate the Auger-electron energies for bismuth we had to use the values for polonium ($Z+1$), which were not included in Sandström's table. In this case, there-

Table 2. Comparison of the experimental lines and their interpretation in earlier investigations.

Interpretations are printed in bold type if they agree with those in the present work. Energy values are given in keV. Transitions ascribed to thallium are denoted by (Tl), the remaining transitions are ascribed to bismuth.

(1) Black 1925	(2) Flam-mersfeld 1939	(3) Butt 1950	(4) Kobayashi 1953	(5) Bashylov *et al.* 1953	(6) Rosenblum *et al.* 1956	(7) Burde & Cohen 1956	(8) Bellicard 1957	(9) Authors 1958
4.29 (?)			4–5 (v.w.) (conv. line ?)					
			5.4 (v.w.) $L_{\mathrm{III}} M_{\mathrm{I}} M_{\mathrm{I}}$			5.48 (v.w.) $L_{\mathrm{III}} M_{\mathrm{I}} M_{\mathrm{II}}$ (Tl)		
			5.7 (v.w.) $L_{\mathrm{III}} M_{\mathrm{I}} M_{\mathrm{II}}$	5.8 (v.w.)		5.66 (v.w.) $L_{\mathrm{III}} M_{\mathrm{I}} M_{\mathrm{II}}$		
						5.95 $L_{\mathrm{III}} M_{\mathrm{I}} M_{\mathrm{III}}$ (Tl)	5.920 (v.w.)	
6.14 (v.w.)			6.1 (?) $\boldsymbol{L_{\mathrm{III}} M_{\mathrm{I}} M_{\mathrm{III}}}$	6.1 (w.)		6.18 (w.) $L_{\mathrm{III}} M_{\mathrm{II}} M_{\mathrm{III}}$ (Tl) $\boldsymbol{L_{\mathrm{III}} M_{\mathrm{I}} M_{\mathrm{III}}}$	6.150 (w.) $L_{\mathrm{III}} M_{\mathrm{II}} M_{\mathrm{III}}$ (Tl)	6.135 (v.w.) $\boldsymbol{L_{\mathrm{III}} M_{\mathrm{I}} M_{\mathrm{III}}}$
					6.20 (w.)		6.200 (w.)	6.197 (?) $L_{\mathrm{III}} M_{\mathrm{II}} M_{\mathrm{III}}$ (Tl)
6.48 (w.)					6.47 (w.)	6.44 (w.) $\boldsymbol{L_{\mathrm{III}} M_{\mathrm{II}} M_{\mathrm{III}}}$	6.435 (w.) $\boldsymbol{L_{\mathrm{III}} M_{\mathrm{II}} M_{\mathrm{III}}}$	6.429 (w.) $\boldsymbol{L_{\mathrm{III}} M_{\mathrm{II}} M_{\mathrm{III}}}$
			6.6 (w.) $\boldsymbol{L_{\mathrm{III}} M_{\mathrm{V}} M_{\mathrm{IV}}}$	6.6 (w.)	6.69 (v.w.)	6.65 (m.) $L_{\mathrm{III}} M_{\mathrm{II}} M_{\mathrm{IV}}$ (Tl)	6.615 (v.w.) $L_{\mathrm{III}} M_{\mathrm{III}} M_{\mathrm{III}}$ (Tl)	6.636 (v.w.) $\boldsymbol{L_{\mathrm{III}} M_{\mathrm{I}} M_{\mathrm{IV}}}$
		6.71 (v.w.) $L_{\mathrm{III}} M_{\mathrm{V}} N_{\mathrm{II}}$ (Tl)					6.735 (v.w.) $L_{\mathrm{III}} M_{\mathrm{II}} M_{\mathrm{V}}$ (Tl)	6.773 (v.w.) $L_{\mathrm{III}} M_{\mathrm{I}} M_{\mathrm{V}}$
7.06 (m.) $L_{\mathrm{III}} M_{\mathrm{II}} M_{\mathrm{V}}$		7.10 (m.) $L_{\mathrm{III}} M_{\mathrm{V}} N_{\mathrm{II}}$	7.0 (w.) $L_{\mathrm{III}} M_{\mathrm{II}} M_{\mathrm{V}}$		7.00 (m.)	7.02 (m.) $\boldsymbol{L_{\mathrm{II}} M_{\mathrm{II}} M_{\mathrm{IV}}}$	6.980 (w.) $L_{\mathrm{III}} M_{\mathrm{II}} M_{\mathrm{V}}$	6.970 (w.) $\boldsymbol{L_{\mathrm{III}} M_{\mathrm{II}} M_{\mathrm{IV}}}$
								7.033 (v.w.) $L_{\mathrm{III}} M_{\mathrm{II}} M_{\mathrm{V}}$
						7.14 (m.) $\boldsymbol{L_{\mathrm{III}} M_{\mathrm{III}} M_{\mathrm{IV}}}$ (Tl)		7.157 (?) $\boldsymbol{L_{\mathrm{III}} M_{\mathrm{III}} M_{\mathrm{IV}}}$ **(Tl)**
					7.19			7.197 (v.w.) $L_{\mathrm{III}} M_{\mathrm{III}} M_{\mathrm{V}}$ (Tl)
			7.5 (m.)	7.2 (s.)	7.49–7.73(m.)	7.49 (m.)		7.434 (m.)

$\boldsymbol{L_{III} M_{III} M_V}$		$L_{III} M_V N_{IV}$ (Tl)					$\boldsymbol{L_{III} M_{III} M_V}$	$\boldsymbol{L_{III} M_{III} M_V}$
						7.62 (s.) $L_{III} M_{IV} M_{IV}$ (Tl)	7.640 (m.) $\boldsymbol{L_{III} M_{IV} M_V}$ (Tl)	7.644 (v.w.) $\boldsymbol{L_{III} M_V M_V}$ **(Tl)** 7.735 (v.w.) $L_{III} M_V M_V$ (Tl) 7.911 (v.w.) $L_{III} M_{IV} M_{IV}$
8.20 (v.s.) $L_{III} M_V M_V$	7.0 (v.s.)	8.10 ± 0.05 (s.) $L_{III} M_V N_{IV}$	8.1 (v.s.) $\boldsymbol{L_{III} M_{IV} M_V}$ $L_{III} M_V M_V$	7.7 (v.s.)	8.08 (v.s.)	8.05 (v.s.) $L_{III} M_{IV} M_{IV}$ 8.14 (w.) $L_{II} M_{II} M_{III}$ (Tl)	8.040 (v.s.) $\boldsymbol{L_{III} M_{IV} M_V}$ 8.145 (s.) $\boldsymbol{L_{III} M_V M_V}$	8.025 (v.s.) $\boldsymbol{L_{III} M_{IV} M_V}$ 8.147 (s.) $\boldsymbol{L_{III} M_V M_V}$ 8.198 (v.w.) $L_{II} M_{II} M_{III}$ (Tl) 8.417 (v.w.) $L_{II} M_I M_{III}$
						8.6 (w.) $L_{II} M_{II} M_{III}$ (Tl)	8.670 (v.w.) $L_{II} M_{III} M_{III}$ (Tl)	
8.72 (v.w.) $L_{III} M_V M_V$ (Pt)			8.7 (v.w.) $L_{III} N_I N_{II,\,III}$	8.4 (w.)	8.82 (m.)	8.71 (w.) $\boldsymbol{L_{II} M_{II} M_{III}}$ 9.06 (s.) $L_I M_I M_{IV}$	8.720 (w.) $\boldsymbol{L_{II} M_{II} M_{III}}$ 8.960 (v.w.) $L_{II} M_I M_V$ 9.140 (v.w.) $\boldsymbol{L_{II} M_{III} M_{IV}}$ (Tl)	8.732 (w.) $\boldsymbol{L_{II} M_{II} M_{III}}$ 8.967 (v.w.) $L_{III} M_I N_V$ 9.120 (v.w.) $\boldsymbol{L_{II} M_{III} M_{IV}}$ **(Tl)**
9.32 (w.) $\boldsymbol{L_{II} M_{II} M_{IV}}$			9.2 (w.) $L_{II} M_{II} M_{IV}$ $L_{III} M_{II} N_V$	9.0 (w.)	9.22 (m.) 9.40 (m.) 9.53 (w.)	9.28 (w.) $\boldsymbol{L_{II} M_{II} M_{IV}}$	9.200 (w.) $\boldsymbol{L_{II} M_{II} M_{IV}}$ 9.305 (w.) $\boldsymbol{L_{II} M_{II} M_V}$ 9.510 (w.)	9.20 (w.) $\boldsymbol{L_{II} M_{II} M_{IV}}$ 9.316 (w.) $\boldsymbol{L_{II} M_{II} M_V}$ 9.499 (w.) $L_{III} M_{II} N_{VI,\,VII}$ $L_{III} M_{III} N_{III}$ 9.585 (v.w.) $L_{II} M_{IV} M_{IV}$ (Tl)

Table 2 *(continued)*

(1) Black 1925	(2) Flam-mersfeld 1939	(3) Butt 1950	(4) Kobayashi 1953	(5) Bashylov *et al.* 1953	(6) Rosenblum *et al.* 1956	(7) Burde & Cohen 1956	(8) Bellicard 1957	(9) Authors 1958
9.85 (m.) $L_{III}\,M_{V}\,N_{I}$ $\boldsymbol{L_{II}\,M_{III}\,M_{IV}}$	8.7 (m.)	9.82 (m.) $L_{III}\,M_{V}\,N_{V}$ (Tl)	9.7 (s.) $\boldsymbol{L_{II}\,M_{III}\,M_{IV}}$ $L_{III}\,M_{III}\,N_{V}$ $L_{III}\,M_{V}\,N_{I}$	9.3 (s.)	9.77 (s.)	9.68 (s.) $L_{III}\,M_{IV}\,N_{IV,V}$ (Tl)	9.735 (m.) $\boldsymbol{L_{II}\,M_{III}\,M_{IV}}$	9.729 (m.) $\boldsymbol{L_{II}\,M_{III}\,M_{IV}}$ $L_{II}\,M_{IV}\,M_{V}$ (Tl)
						9.68 (w.) $L_{I}\,M_{I}\,M_{IV}$		9.878 (v.w.) $L_{I}\,M_{II}\,M_{IV}$
								9.998 (v.w.) $L_{I}\,M_{II}\,M_{V}$
						10.07 (v.w.)		10.087 (v.w.) $L_{III}\,M_{V}\,N_{VI,VII}$(Tl)
					10.28 (s.)	10.21 (s.) $L_{III}\,M_{IV}\,N_{IV,V}$	10.260 $\boldsymbol{L_{II}\,M_{IV}\,M_{IV}}$	10.223 (m.) $\boldsymbol{L_{II}\,M_{IV}\,M_{IV}}$
10.44 (v.s.) $L_{III}\,M_{V}\,N_{V}$ $\boldsymbol{L_{II}\,M_{IV}\,M_{V}}$ $L_{II}\,M_{IV}\,M_{IV}$ $L_{III}\,M_{V}\,N_{V}$ (Pt)	9.7 (m.)	10.39 (v.s.) $L_{III}\,M_{V}\,N_{V}$	10.3 (s.) $\boldsymbol{L_{II}\,M_{IV}\,M_{IV,V}}$ $L_{III}\,M_{IV}\,N_{V}$ $L_{III}\,M_{V}\,N_{IV,V}$	9.5 (s.)	10.37 (v.s.)	10.27 (m.) $L_{I}\,M_{IV}\,M_{IV}$ (Tl)	10.340 $\boldsymbol{L_{II}\,M_{IV}\,M_{V}}$	10.315 (v.s.) $\boldsymbol{L_{II}\,M_{IV}\,M_{V}}$
								10.423 (v.w.) $L_{II}\,M_{V}\,M_{V}$
								10.547 (v.w.) $L_{III}\,M_{IV}\,N_{VI,VII}$
10.71 (w.) $L_{III}\,M_{III}\,O$				10.4 (m.)	10.63 (m.)	10.7 (v.w.) $L_{I}\,M_{IV}\,M_{IV}$	10.650 (v.w.)	10.643 (m.) $L_{III}\,M_{V}\,N_{VI,VII}$
					10.79 (w.)			10.761 (v.w.)
11.14 (w.) $L_{II}\,M_{I}\,N_{IV}$			11.0 (w.) $L_{II}\,M_{I}\,N_{IV}$ $L_{III}\,M_{V}\,O$ or conv. line 27.4 or 15 keV	11.1 (w.)	11.01 (m.)	11.02 (w.) $L_{II}M_{III}\,N_{II}$ (Tl)	10.030 (v.w.)	10.996 (w.) $L_{I}\,M_{IV}\,M_{V}$
					11.16 (w.)			
					11.27 (w.)	11.2 (v.w.) $\boldsymbol{L_{II}\,M_{I}\,N_{IV,V}}$		11.257 (w.) $\boldsymbol{L_{II}\,M_{I}\,N_{V}}$
					11.53 (m.)	11.52 (v.w.)	11.515 (v.w.)	11.529 (w.)

			(v.w.)			**$L_{II} M_{III} N_{II}$**		**$L_{II} M_{III} N_{II}$**
					11.87			11.874 (v.w.)
								$L_{I} M_{I} N_{IV}$
						11.93 (w.)		11.999 (v.w.)
						$L_{II} M_{V} N_{IV,V}$ (Tl)		$L_{II} M_{III} N_{IV}$
								12.141 (w.)
								$L_{II} M_{V} N_{I}$
								$L_{III} N_{II} N_{V}$
12.37 (v.w.)		12.26 (w.)		12.2 (w.)	12.27 (w.)	12.22 (v.w.)	12.260 (v.w.)	12.289 (w.)
$L_{II} M_{IV} N_{III}$		$L_{II} M_{IV} N_{II}$				$L_{II} M_{IV} N_{II}$	$L_{II} M_{IV} N_{III}$	$L_{III} N_{I} N_{VI,VII}$
12.66 (v.w.)	11.8 (v.w.)	12.62 (w.)	12.6–13.5 (v.w.)		12.51 (s.)	12.42 (v.w.)	12.500 (w.)	12.462–12.518 (m.)
$L_{II} M_{IV} N_{V}$		$L_{II} M_{IV} N_{VI}$				$L_{I} M_{IV} N_{IV,V}$ (Tl)	$L_{II} M_{IV} N_{IV}$	
$L_{II} M_{IV} O$						12.61 (v.w.)		12.581 (w.)
$L_{II} M_{V} N_{IV}$						**$L_{II} M_{V} N_{IV,V}$**		**$L_{II} M_{V} N_{IV}$**
					12.78 (w.)			12.793 (w.)
								$L_{III} N_{V} N_{VI,VII}$
								$L_{II} M_{IV} N_{VI,VII}$
					12.95 (w.)			12.972 (v.w.)
								$L_{I} M_{III} N_{VI,VII}$
					13.24 (v.w.)			
				13.6 (w.)	13.51–14.23			13.855 (v.w.)
					(v.w.)			$L_{II} N_{IV} N_{IV,V}$ (Tl)
								$L_{II} N_{V} N_{V}$ (Tl)
								14.091 (v.w.)
								14.163 (v.w.)
					14.43 (v.w.)			14.465 (v.w.)
								14.656 (v.w.)
				14.3 (w.)	14.76 (w.)			14.746 (w.)
								$L_{II} N_{IV} N_{IV,V}$
								$L_{II} N_{V} N_{V}$
			15.0–16.0					15.574 (w.)
			conv. line					
			31–32 keV					

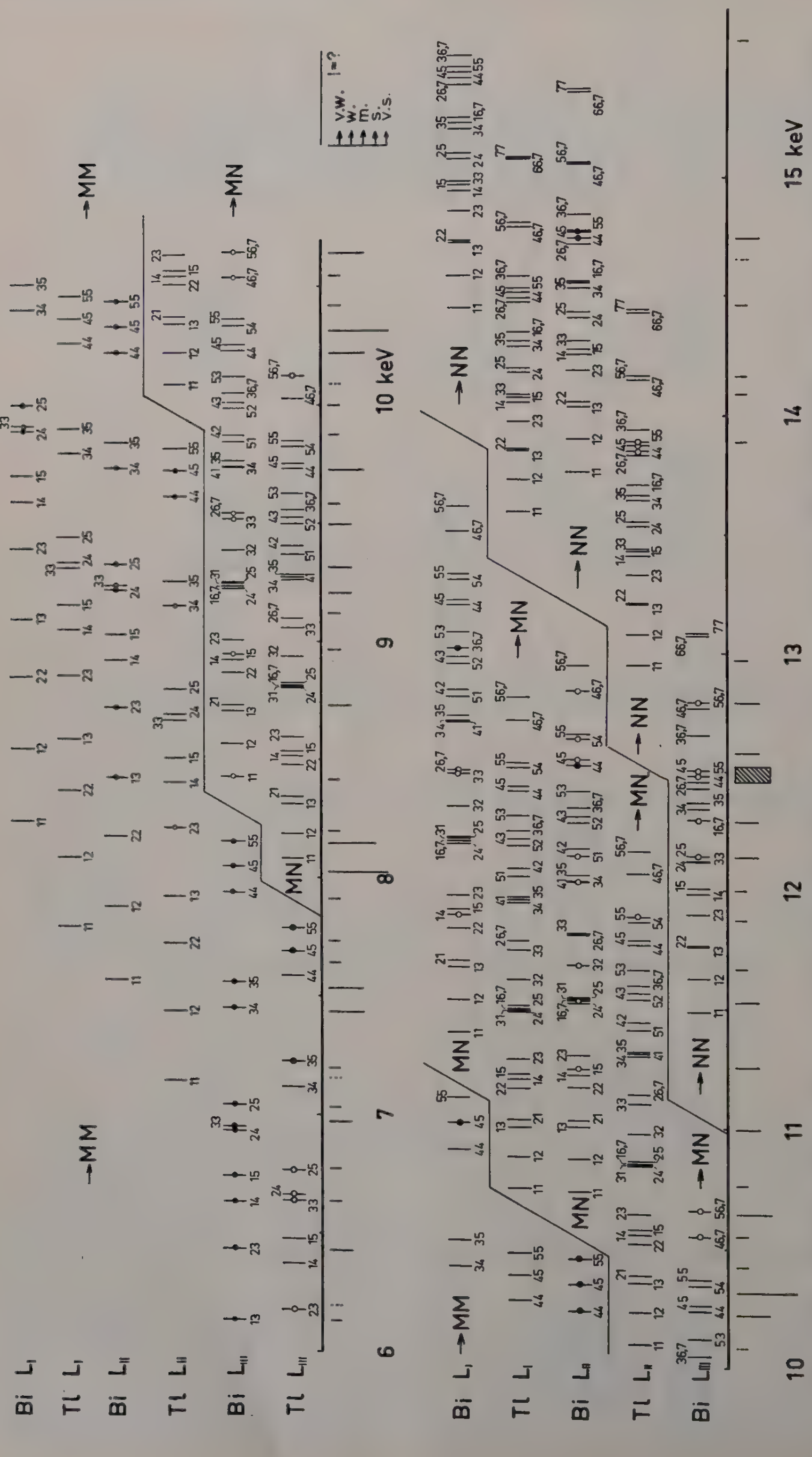

Fig. 4. The possible *LMM*, *LMN*, and *LNN* energies (computed for W_{Z+1}) compared with the energies of the experimentally found Auger lines. The theoretical configuration, chosen by us, is marked with a heavy point. In doubtful cases the lines are marked with an open circle. See the text to Fig. 1.

fore, we used also the table by Hill *et al.* [21] in such a way that we calculated the energy differences between corresponding shells in polonium and bismuth according to Hill *et al.* and then added this difference to the corresponding ionization energy for bismuth according to Sandström.

The positions of the lines found by different authors are generally in a good agreement—to the extent, at least, that one can easily find the correspondance—with exception of the results of Flammersfeld and those of Bashylov *et al.* Therefore the results of these authors are compared in Table 2 with those of others according to the intensity ratios rather than to energy only.

As regards the results of the present work it must be added that the positions of the very weak lines should not be considered to be as certain as those of the majority ot the other lines. Especially the thallium lines, being in general much more diffuse, are determined with somewhat worse accuracy. The maximum error of the energy values, taken as the sum of the errors of the determination of the line position in the plate, or rather in the copy of the plate (this error is by far the largest), and of the distance sample–calibration edge in the filmholder is, for an energy of about 8 keV and for not very weak and diffuse lines, about ±15 eV. The errors for not very weak lines probably do not exceed ±10 eV in the neighbourhood of 8 keV. On the other hand for very weak lines the error in energy might be up to ±20 keV.

Interpretation of the lines recorded

A thorium B source in equilibrium with its decay products contains the elements $Z = 81$ (Tl), 82 (Pb), 83 (Bi) and 84 (Po). However, the contribution to the K and L shell vacancies due to internal conversion of gamma-rays is, according to for instance Flammersfeld [7], absolutely negligible in the case of polonium and to a good approximation negligible also for lead.

The strong internal conversion lines belong to transitions for which we here give names after the most prominent corresponding conversion lines according to Ellis' notation, namely γF ($=239$ keV, the K-line of which is the well known F-line, $L_1 = I$ and so on), γE ($=115$ keV, $L_1 = E$) and γH ($=299$ keV, $K = H$) in Bi^{212} and γA ($=40$ keV, $L_1 = A$) in Tl^{208}. As the intensity measurements of the internal conversion lines due to these transitions (Surugue [22], Flammersfeld [7]) are not of very high accuracy and also not consistent,[1] it was decided to use in the further discussion the theoretical conversion coefficients for the γF, γE and γA lines (assuming they are pure magnetic dipole transitions [24, 27, 28] and to estimate roughly only the contributions from the other lines, using the corrected decay scheme of ThB (Fig. 5). This scheme is mainly in accordance with that given by Hollander *et al.* [23]. The only change concerns the intensity of the γE-transition, which according to Hollander *et al.* is 2 %. We consider this to be too low. Assuming the γE-transition is a pure magnetic dipole [24] the conversion coefficients with correction for the finite nuclear size [25] are $K_{\beta_1} = 6.21$, $L_{\mathrm{I}\beta_1} = 0.92$, $L_{\mathrm{II}\beta_1} = 0.087$, $L_{\mathrm{III}\beta_1} = 0.006$.

If we take the γE-transition intensity equal to 2 % the distribution (per 1 disintegration of ThB) of the primary vacancies due to this transition will be:

---

[1] As an example of such inconsistencies we can cite the intensity of the A-line in the β-spectrum of ThB + C + C″. According to Surugue [22] the intensity ratio of the $A + A\alpha$ line to, for instance, the F-line, is 33:100, while according to Flammersfeld [7] the same ratio is 20.9:28.4 = 0.74. Using the scheme of Fig. 5 and computing the conversion coefficients we get for this ratio 84.6:120.6 = 0.70 in quite good agreement with Flammersfeld.

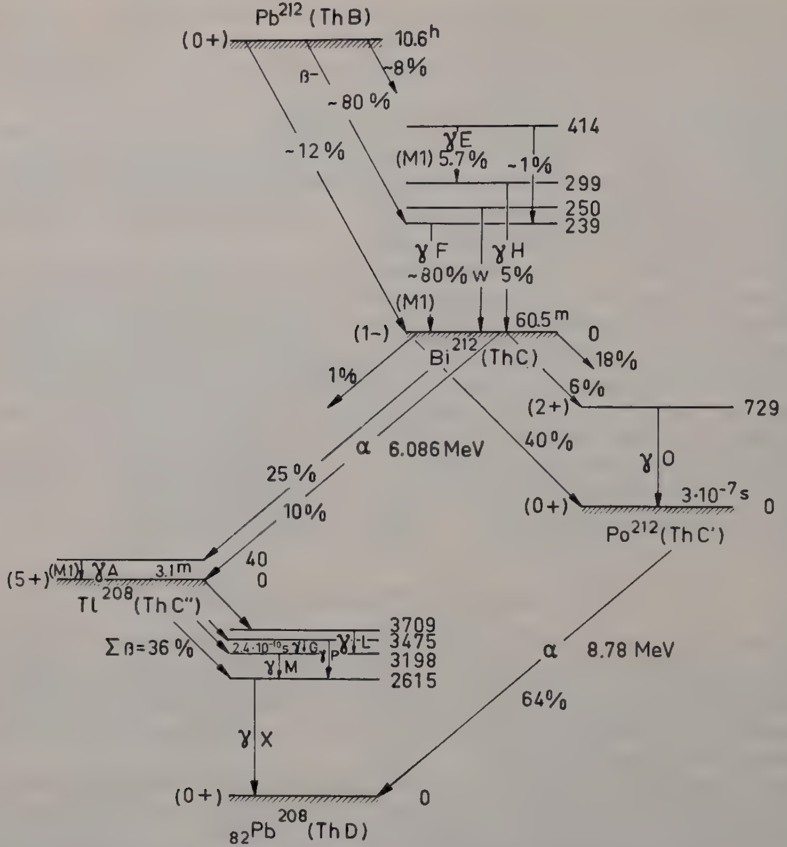

Fig. 5. The decay scheme of ThB (Pb^{212}), mainly in accordance with Strominger, Hollander, and Seaborg [23].

$$K \text{ shell} = 0.0176, \quad L_{\mathrm{I}} \text{ shell} = 0.0023, \quad L_{\mathrm{II}} \text{ shell} = 0.000247,$$

while similar considerations for the γF-transition (80 %) give the following contribution from this transition:

$$K \text{ shell} = 0.335, \quad L_{\mathrm{I}} \text{ shell} = 0.050, \quad L_{\mathrm{II}} = 0.00474.$$

The ratio of the L_{I} conversion lines, i.e. the well known I and E lines in the ThB β-spectrum, is for these computed values $0.050:0.0023 = 21.7$ while experimentally it is $22:3.4 = 6.5$ (Surugue [22]) or $5.13:0.63 = 8.1$ (Flammersfeld [7]; this is the ratio of total L-conv. lines, i.e. $(I + Ia)/(E + E_a)$). Comparing these values we get for the γE-transition intensity 6.8 % from the data of Surugue and 5.3 % from those of Flammersfeld. A similar discussion for the conversion line from the L_{II} shell (E_a-line) gives us a γE-line intensity of 3.67 %, but of course the intensity data for so weak lines are more uncertain. The ascribing of such a low intensity to the γE-transition in Bi^{212} spectrum is due to the fact that the K-conversion line from this transition was measured with a very low accuracy as this line was strongly masked by the A-line

Table 3. Distribution of the primary vacancies in bismuth and thallium (per 1 disintegration of ThB).

	Shell	L_I	L_{II}	L_{III}	K
$_{83}$Bi	Vacancies after conversion of the γF-transition	0.050	0.0047	negligible	0.335
	Vacancies after conversion of other γ-transitions	0.008	0.0006	negligible	0.064
	Total	0.058	0.0053	negligible	0.399
	Total after K-X-transitions	0.058	0.109	0.212	—
$_{81}$Tl	Vacancies after conversion of the γA-transition	0.215	0.020	0.002	—

in the β-spectrum of ThB+C+C″. It was even pointed out by Wapstra and Nijgh [24] as an example of the anomalies in the internal conversion coefficients.

Recently, however, Nielsen *et al.* [26] measured the intensity of this line by the coincidence method and found that it was 19 ± 3 % of that of the A line. From this we obtain for the intensity of the γE-transition the value 5.73 %, which is in a very good agreement with the calculations. Taking the γE-transition intensity equal to 5.7 % we do not make any effort to see if it will change the intensities acsribed to the other γ-transitions from the higher excited levels in ThC. In further discussion only the intensities of the γF- and the γE-transitions in ThC are used.

The L-shell vacancies are formed either due to direct L-shell internal conversion of γ-rays or due to the K-shell internal conversion, which leads then to the L-ionisation by an X-ray or an Auger process. According to Massey and Burhop [29] the $K\alpha_1$ and $K\alpha_2$ X-rays, leading to the ionization in the L_{III} and L_{II} shells, amount to 53 % and 26 % respectively of all transitions to the K-shell. 4.3 % of the K-shell vacancies are, according to Mladjenovic and Slätis [30], transferred to the L-shell by the Auger process. This process, however, leads to atoms doubly ionized in LL (2.6 %) or LM (1.7 %) subshells and thus the energy of L-Auger electrons eventually emitted from such atoms would differ significantly from that of the electrons emitted from atoms singly ionized in the inner shells. The intensity of these electrons is perhaps too low for giving detectable lines. Table 3 shows the distribution of the primary vacancies in bismuth and thallium obtained in the way described above, excluding the vacancies from the K-Auger transitions.

In the atomic number region considered ($Z = 81$ and 83, respectively) there is energetically possible a special kind of Auger transition between the subshells of the same electron shell, namely of the $L_I \rightarrow L_{III} M_{IV,V}$ and $L_I \rightarrow L_{II} N_{\geq IV}$ type. This was at first pointed out by Coster and Cronig (1935) [31] and then confirmed by many authors [1]. Very strong arguments for such transitions are given by the experiments on the X-ray satellites. For example the curve representing the intensity of the L_α satellites versus Z measured by Shrader and reproduced by Cooper [32] shows a maximum about $Z = 80$ (then slowly decreases) and agrees well with the predictions based on energetical considerations. Ross *et al.* [33] analyzed the experimental data available on the L-fluorescent yields and X-rays satellites for bismuth (RaE) and found the following values for the two possible types of Coster–Kronig transitions:

Table 4. Distribution of the L-vacancies in Bi and Tl per disintegration of ThB.

(a) Vacancies after internal conversion of L-lines and, for Bi, after filling of K-shell vacancies with electrons from the L-shell.

(b) Single vacancies after Koster–Cronig transition.

(c) Vacancies in atoms additionally ionized in the M- or N-shell by this Koster–Cronig transition.

Element		Shell		
		L_I	L_{II}	L_{III}
$_{83}$Bi	a	0.058	0.109	0.212
	b	0.014	0.109	0.212
	c	—	0.014	0.030
	c/b	0	0.13	0.14
$_{81}$Tl	a	0.215	0.020	0.002
	b	0.052	0.020	0.002
	c	—	0.052	0.112
	c/b	0	2.6	56

$$L_I \to L_{II}N; \quad f_{12} = 19\,\%$$
$$L_I \to L_{III}M; \quad f_{13} = 58\,\%.$$

These values were taken as the mean from different experiments that were not in very good consistence among themselves and therefore they may suffer from significant errors. Following the discussion by Ross *et al.* [33] we assume that the probability of the $L_{II} \to L_{III}N$ transition is negligible.

Recently Burde and Cohen [12] computed the factors f_{12} and f_{13} from their experiments on the L-Auger electrons only. The values given by them, being the mean for thallium and bismuth (with the assumption that the difference for these neighbouring elements should be very small) are:

$$f_{12} = 24\,\%, \quad f_{13} = 52\,\%.$$

The distribution of the vacancies after Coster–Kronig transition (using the coefficients of Burde and Cohen) is given in Table 4. It should be mentioned that as a result of a Coster–Kronig transition an atom becomes doubly ionized and the energy of an Auger-electron emitted from it will therefore differ from that for singly ionized atoms. In the case of bismuth this effect will cause a very weak "satellite" of lower energy, the maximum energy difference being of the order of magnitude $\Delta E = W(Z+2) - W(Z+1)$ for a satellite of the Auger line LVW. For the L_{II} and L_{III} Auger lines the intensity of this satellite is at the most 13 to 14 per cent of the mean line. Such satellites are either not observed on our plates, or are coincident with other lines. In the case of thallium, however, the Coster–Kronig transition will predominate (Table 4). The experimental lines should then have a little lower energy than the theoretical ones (computed without the maximum correction ΔE above). This seems also to happen in some cases (compare for instance the corresponding Bi- and Tl-groups $L_{III}M_{IV}M_{IV}$, $L_{III}M_{IV}M_V$, $L_{III}M_VM_V$ in Figs. 3 and 4). For the thallium L_{II}-lines the transitions belonging to Coster–Kronig transitions are 2.6 times more probable than those in singly ionized atoms and hence of comparable intensity, which should give reason to a broadening of the thallium L_{II}-lines. The thallium lines are more diffuse than the corresponding bismuth lines also for another reason (see below).

It is seen from Tables 3 and 4 that the intensities of the Auger lines for bismuth and for thallium should be similar or, at least, comparable. Figs. 4 and 5 show, however, that none of the more probable configurations of thallium lines corresponds to any of the stronger experimental lines and, moreover, that only for the strongest lines for bismuth one can find the corresponding lines for thallium, usually very weak and broadened. On the other hand there are no thallium lines where the corresponding bismuth lines are not much stronger.

This appears to be reasonable when one takes into account the fact that the Auger electrons from thallium are emitted after the Bi^{212} (ThC) α-transition, which cause a recoil of the residual thallium nuclei. The Doppler effect due to this recoil causes so large broadening of the lines that in our high resolution spectrometer very weak lines may completely disappear and stronger ones are to be seen only as very weak bands.

The recoil energy of a Tl^{208} nucleus after the 6.16 MeV α-transition from Bi^{212} is about 118 keV. Then the Doppler effect for a 10 keV electron is about ± 112 eV. If we assume there is no angular correlation between the Auger electrons and the α-particles we should get in this energy region bands of a width larger than 200 eV. The contribution from the electrons emitted from the atoms recoiled into the source or the source backing, however, may be considerably changed. Graham and Bell [34] estimated the upper limit of the half-life of the 40 keV level in thallium as 7×10^{-11} sec. From the recoil broadening of the internal conversion lines Burde and Cohen [35] were able to determine this time as $(1.0 \pm 0.5) \times 10^{-12}$ sec. The initial velocity of a recoil nucleus is about 3.3×10^{7} cm/sec. Thus most of the nuclei recoiled into the source will be slowed down if not stopped before a conversion electron will be emitted, so that the Doppler effect for these electrons will not be so great. (The time of the emission of the Auger electrons after the conversion electron is extremely short. Estimated from the level width it is for the L-Auger electrons of the order of 10^{-16} sec. (see, for instance, ref. [36]). Hence in these considerations we can assume those two processes to be almost simultaneous.) On the other hand these electrons have to traverse some path in the source backing—up to about 100 atom layers—and the losses of their energy due to absorption all have values between zero and a certain maximum. This maximum is, for instance, for 10 keV electrons of the order of magnitude 50 eV. Therefore this recoil absorption effect will also give reason to the broadening of the thallium Auger lines.

All the lines identified by us as thallium Auger lines are very broad indeed, although it is difficult to determine the broadening of such very weak lines in a photographic emulsion. It is also very satisfactory that the positions of these lines are generally in a relatively good agreement with those of the strong thallium lines found by Burde and Cohen [12], who measured the thallium Auger-electrons spectrum separately, in coincidence with the alpha-particles. Due to the character of their experiment these authors had the shift in the energy in one direction only (toward higher energies) and they were able to make the correction for the recoil. It may be mentioned also that measured with lower resolution these diffuse lines become more prominent.

SUMMARY

1. A brief review of earlier works on L-Auger lines in the beta-ray spectrum of $\mathrm{ThB}+\mathrm{C}+\mathrm{C}''$ is given.

2. The L-Auger lines in the beta-spectrum of the thoron active deposit were recorded photographically in a permanent magnet beta-ray spectrometer at a high resolution (<1 promille). 54 lines were found in the energy region 6–16 keV.

3. A comparison of the position of these lines with the L-Auger lines found by earlier workers is given schematically.

4. 47 lines were interpreted. The majority of the L-Auger lines belong to ThC (Bi^{212}), the rest are due to ThC″ (Tl^{208}).

5. The higher the resolution, the weaker (more diffuse) the thallium lines, because these arise from thallium nuclei recoiling after the α-emission of the parent nuclei ThC. The influence of the Coster–Kronig transition on the intensity of the lines is discussed.

6. The decay scheme of $\mathrm{ThB}+\mathrm{C}+\mathrm{C}'+\mathrm{C}''$ is considered and some corrections are introduced.

ACKNOWLEDGEMENTS

We would like to thank Professor Manne Siegbahn for his interest in this work and for the hospitality of the Nobel Institute extended to the first-named author during his stay in Stockholm.

Nobel Institute of Physics, Stockholm 50, Sweden.

REFERENCES

1. E. H. S. Burhop, The Auger Effect and other Radiationless Transitions. Cambridge, University Press, 1952.
2. I. Bergström and R. D. Hill, Arkiv f. Fysik *8*, 21–26 (1954).
3. M. Ference, Jr., Phys. Rev. *51*, 720 (1937).
4. E. Sokolowski, C. Nordling, and K. Siegbahn, Arkiv f. Fysik *12*, 301–318 (1957).
5. I. Bergström, Auger electrons emitted from radiactive atoms, in "Beta- and Gamma-Ray Spectroscopy", ed. by K. Siegbahn, Amsterdam, 1955.
6. D. H. Black, Proc. Camb. Phil. Soc. *22*, 838 (1925).
7. A. Flammersfeld, Z. Phys. *114*, 227 (1939).
8. D. K. Butt, Proc. Phys. Soc. *63A*, 986 (1950).
9. Y. Kobayashi, Journal Phys. Soc. Japan *8*, 440 (1953).
10. A. A. Bashylov, B. S. Dzelepov, and L. S. Czervinskaya, Izvestia Akademii Nauk, SSSR, Ser. Fiz., *17*, 428 (1953).
11. S. Rosenblum, J. Sant'Ana Dionisio, M. Valadares, Journal Phys. Radium. *17*, 112 (1956).
12. J. Burde and S. G. Cohen, Phys. Rev. *104*, 1085 (1956).
13. J. B. Bellicard, Annales de Physique *2*, 419 (1957).
14. H. Slätis, Nucl. Instr. *2*, 332 (1958).
15. B. Gauthé and J. M. Blum, Compt. Rend. Acad. Sci. (Paris) *234*, 2189 (1952).
16. Beta- and Gamma-Ray Spectroscopy, ed. by K. Siegbahn, Amsterdam, 1955, Appendix VII.
17. H. Slätis, Arkiv f. Fysik *6*, 415 (1953).
18. Landolt-Börnstein, 6. Auflage, 5. Teil, Berlin–Göttingen–Heidelberg, Springer-Verlag, 1952.
19. E. R. Cohen, J. W. M. DuMond, T. W. Layton, and J. S. Rollet, Rev. Mod. Phys. *27*, 363 (1955).
20. A. E. Sandström, Handbuch d. Physik, Vol. 30 (1957), pp. 78–245 (Table 27).
21. R. D. Hill, E. L. Church, and J. W. Mihelich, Rev. Sci. Instr. *23*, 523 (1952).
22. M. J. Surugue, Ann. Phys. *8* (11th Series), 484 (1937).
23. D. Strominger, J. M. Hollander, and G. T. Seaborg, Table of Isotopes (Rough Draft), U.C.R.L. (1957), private communication.

24. A. H. Wapstra and G. J. Nijgh, Nucl. Phys. *1*, 245 (1956).
25. M. E. Rose, Internal Conversion Coefficients (1957), private communication.
26. K. O. Nielsen, O. B. Nielsen, and M. A. Waggoner, Nucl. Phys. *2*, 476 (1956/57).
27. J. W. Horton, Phys. Rev. *101*, 717 (1956).
28. J. W. Weale, Proc. Phys. Soc. *68 A*, 35 (1955).
29. H. S. W. Massey and E. H. S. Burhop, Proc. Camb. Phil. Soc. *32*, 461 (1936).
30. M. Mladjenovič and H. Slätis, Arkiv f. Fysik *9*, 41 (1955).
31. D. Coster and R. Kronig, Physica *2*, 13 (1935).
32. J. N. Cooper, Phys. Rev. *61*, 234 (1942).
33. M. A. S. Ross, A. J. Cochran, J. Hughes, and N. Feather, Proc. Phys. Soc. (London), *68 A*, 612 (1955).
34. R. L. Graham and R. E. Bell, Can J. Phys. *31*, 374 (1953).
35. J. Burde and S. G. Cohen, Phys. Rev. *104*, 1093 (1956).
36. J. N. Cooper, Phys. Rev. *65*, 155 (1944).
37. J. Tousset et A. Moussa, J. Phys. et Rad. *19*, 39 (1958).

Note added in proof. — The authors would like to point out that in giving a review of the previous investigations and comparing the results they have overlooked the last work on the same subject by C. Geoffrion and G. Nadeau (Can. J. Phys. 36, 1284–31, Nov. 1957).

Tryckt den 2 september 1958

Uppsala 1958. Almqvist & Wiksells Boktryckeri AB